

# Optics Letters

## Low helium permeation cells for atomic microsystems technology

ARGYRIOS T. DELLIS,<sup>1,\*</sup> VISHAL SHAH,<sup>2</sup> ELIZABETH A. DONLEY,<sup>1</sup> SVENJA KNAPPE,<sup>1</sup> AND JOHN KITCHING<sup>1</sup>

<sup>1</sup>National Institute of Standards and Technology, Boulder, Colorado 80305, USA

<sup>2</sup>QuSpin Inc., 2011 Cherry Street, Unit 112, Louisville, Colorado 80027, USA

\*Corresponding author: argyrios.dellis@nist.gov

Received 26 February 2016; revised 14 May 2016; accepted 15 May 2016; posted 16 May 2016 (Doc. ID 260086); published 9 June 2016

**Laser spectroscopy of atoms confined in vapor cells can be strongly affected by the presence of background gases. A significant source of vacuum contamination is the permeation of gases such as helium (He) through the walls of the cell. Aluminosilicate glass (ASG) is a material with a helium permeation rate that is many orders of magnitude lower than borosilicate glass, which is commonly used for cell fabrication. We have identified a suitable source of ASG that is fabricated in wafer form and can be anodically bonded to silicon. We have fabricated chip-scale alkali vapor cells using this glass for the windows and we have measured the helium permeation rate using the pressure shift of the hyperfine clock transition. We demonstrate micro fabricated cells with He permeation rates at least three orders of magnitude lower than that of cells made with borosilicate glass at room temperature. Such cells may be useful in compact vapor-cell atomic clocks and as a micro fabricated platform suitable for the generation of cold atom samples.** © 2016 Optical Society of America

**OCIS codes:** (120.0120) Instrumentation, measurement, and metrology; (130.0130) Integrated optics; (140.0140) Lasers and laser optics; (160.0160) Materials; (220.0220) Optical design and fabrication; (300.0300) Spectroscopy.

<http://dx.doi.org/10.1364/OL.41.002775>

Alkali vapor cells are widely used in experimental atomic physics precision instrumentation such as atomic clocks [1] and magnetometers [2], and for the creation of laser-cooled atoms. The presence of background gas in the cell can change dramatically the properties of the co-located alkali atoms. For example, in buffer-gas cells used in atomic clocks, changes in the buffer gas density cause fractional pressure shifts of the hyperfine “clock” transition on the order of  $10^{-7}$ /Torr, implying that micro Torr-level changes in background pressure can cause observable frequency drifts of the clock frequency at the  $10^{-13}$  level [3]. For laser-cooled systems, the presence of a background gas above about  $10^{-7}$  Torr at room temperature effectively prevents significant numbers of cold atoms from being trapped and shortens the lifetime of atoms that are trapped.

Among the most problematic of residual gases is helium (He) because it permeates readily through most types of glass even at room temperature [4] and is not pumped by passive pumping techniques (e.g., getter pumps). Hence, if its presence in a cell is problematic, it must either be actively pumped away using, for example, an ion pump, or prevented from entering in the first place [5]. Helium permeation is one of the reasons ion pumps are used in almost all cold atom systems. Helium permeation has also been studied as a cause of frequency drifts in vapor cell atomic clocks for some time [6,7]. The use of aluminosilicate glass (ASG) as the cell wall material has been suggested to reduce this drift [8]. Aluminosilicate glass is known to have He permeation rate orders of magnitude lower than borosilicate glass [4], and hence can successfully prevent the He from entering the cell [5]. Helium can also diffuse out of vapor cells and so ASGs are often used in large glass-blown cells in He NMR experiments [9].

Micro fabricated alkali vapor cells [10] have enabled a new generation of miniaturized atomic clocks and magnetometers, now achieving commercial availability. These cells have generally made use of borosilicate glass for the cell windows; borosilicate glass suitable for anodic bonding is available in wafer form. There is current interest to use such cells for experiments and instruments based on laser-cooled atoms [11], in order to reduce their size, power dissipation, and cost. While micro fabricated ion pumps [12] could possibly be used to achieve the required high-vacuum levels, all such pumps demonstrated so far for high vacuum require the use of magnetic fields, which are in close proximity to the atomic sample and are likely to affect the performance of the final instrument. A second approach is to use passive pumping but prevent He from entering the cell using low-permeability glasses. Unfortunately, not all of them are produced in wafer form and even fewer can be anodically bonded to silicon. Recently, the diffusion of Ne in glass has been studied in a micro fabricated alkali vapor cell and novel method for measuring the permeation rates through glasses was suggested [13]. We follow a similar method here in determining the permeation rates of He and verifying that we achieve low He permeation rates in certain cells.

We have identified a suitable type of ASG that is available in wafer form and can be anodically bonded to silicon (SD2 glass from Hoya Corporation [14]). Moreover, we have successfully

fabricated micro machined  $^{87}\text{Rb}$  alkali vapor cells using this type of glass as the optical windows, and have measured the permeation rate using the pressure shift of the hyperfine clock transition. The permeation rate of the ASG under test is at least 1,000 times lower than that of Pyrex. This may suggest that ASG can be used along with nonevaporable getters for fabricating chip-scale cells that may be suitable for cold-atom microsystems. In addition, the anodic bonding process [10,15] used here for fabricating the cells avoids the well-known difficulties of glassblowing this type of glass (such as higher melting temperature, more difficulty in shaping than borosilicate glass, and bubble formation during glass blowing). The anodic bonding procedure we follow is the one described in [10], and the conditions are the same for both Pyrex and ASG.

The diffusion of He in and through glass has been well studied experimentally and theoretically. In many cases, one is interested in the increase of pressure inside a vacuum chamber due to the diffusion of gases from the external environment in the chamber. In the case of a chamber of volume  $V$ , having a glass window of area  $A$  and thickness  $d$ , and assuming that the rest is impermeable to gases, one obtains for the pressure increase [16,17]

$$\Delta P(t) = \frac{AK}{Vd} P_e \left\{ \left( 1 - \frac{P_i}{P_e} \right) (t - t_1) - \left( 2 \sum_{m=1}^{\infty} \frac{(-1)^m - \frac{P_i}{P_e}}{m^2} e^{-m^2 t/t_R} + 4q \sum_{m=0}^{\infty} \frac{1}{(2m+1)^2} e^{-(2m+1)^2 t/t_R} \right) t_R \right\}, \quad (1)$$

where  $P_e$  is the pressure of the gas outside the vacuum chamber,  $P_i$  is the initial pressure of the gas in the chamber, and  $q$  is the ratio of the initial gas concentration in the glass to the maximum concentration that can be achieved ( $q = 0$  for a complete degassed material and  $q = 1$  for a saturated material).  $t_1 = \frac{P_e}{P_e - P_i} \left( 1 + 2 \frac{P_i}{P_e} - 3q \right) \frac{d^2}{6D}$  is the characteristic time needed to establish a constant flow.  $t_R = \frac{d^2}{\pi^2 D}$  is the characteristic time needed for the average concentration of gas inside the glass to reach the value  $S(P_e + P_i)/2$ . Finally,  $K = DS$  is the permeation rate,  $D$  is the diffusion constant following the Arrhenius equation  $D = D_0 e^{-E_D/k_B T}$  ( $T$  is the temperature,  $D_0$  is the maximum diffusion coefficient, and  $E_D$  is the activation energy of the material), and  $S$  is the solubility. In the special case where the glass is completely degassed, ( $q = 0$ ),  $P_i \ll P_e$  and  $t \gg t_R$ . Equation (1) reduces to  $\Delta P(t) = \frac{AK}{Vd} P_e \left( t - \frac{d^2}{6D} \right)$  [11,17]. Equation (1) can be used to determine the pressure,  $P(t)$ , inside the chamber for early times where  $P(t) \ll P_e$ , and in this case  $P(t) \approx P_i + \Delta P(t)$ .

Different methods exist for measuring the permeation of helium through a membrane [4,18]. Usually, a container made out of the material under test is filled with He and then placed inside a vacuum system. By monitoring the pressure in the vacuum system, one can determine if He diffused out of the container. A more sensitive method involves a mass spectrometer for detecting He atoms. We have used a method based on the buffer-gas pressure dependence on the ground state hyperfine splitting of alkali atoms [13]. The experimental arrangement (Fig. 1) is similar to the one used for coherent population trapping (CPT) atomic clocks [19]. The only difference is that the atomic sample is placed inside a vacuum chamber containing He. The vapor cell is made of silicon and glass. The silicon part is etched and two glass windows are anodically bonded to

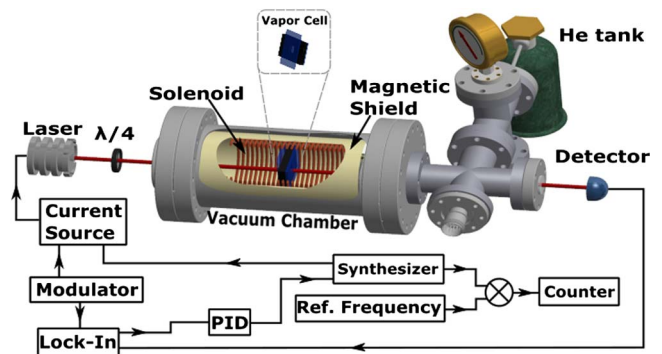


**Fig. 1.** The cell, the heating system, the solenoid providing the longitudinal field, and the magnetic shield are placed inside a vacuum chamber filled with He. A laser beam from a vertical-cavity surface-emitting laser (VCSEL) passes through the cell, and the signal is detected by a photo-diode. The power of the laser is  $75 \mu\text{W}$  and is not actively stabilized. The optical frequency of the laser was locked to the desired atomic transition and modulated using a frequency synthesizer at a frequency equal to the ground state hyperfine splitting of  $^{87}\text{Rb}$ . This signal is used to stabilize the radio frequency of the synthesizer to the atomic resonance. The frequency of the synthesizer is beaten against a stable reference frequency, and the result is recorded by a frequency counter.

the silicon to form a sealed cavity. Prior to bonding the second window,  $^{87}\text{Rb}$ ,  $\text{N}_2$  and Ar are admitted into the cavity (the cavity length is 2 mm long; each window is 0.7 mm thick and has a surface area of  $(3 \text{ mm} \times 3 \text{ mm})$ ; and each cell was filled with 77 Torr of Ar and 125 Torr of  $\text{N}_2$ ). Changes in the buffer-gas pressure and composition affect the CPT resonance frequency. For example, the frequency shift for the hyperfine ground state of  $^{87}\text{Rb}$  from He is  $\beta/\nu_0 = 108.9 \times 10^{-9} \text{ Torr}^{-1}$  [20]. Thus, if He atoms diffuse in the cell, then a drift in the recorded clock frequency would be observed. We can estimate the minimum leak rate that can be measured using this method in a cell of volume  $1 \text{ mm}^3$ . The measured long-term drift in clocks based on these cells is  $\sim 1 \times 10^{-10}/\text{month}$  [21], which corresponds to a minimum measurable leak rate of  $\sim 10^{-18} \text{ Torr m}^3/\text{s}$ .

We measured the clock frequency as a function of time for two different cells. The first cell had windows made of Pyrex and the second cell had windows made of ASG. In both cases the vacuum chamber was initially empty and then filled with He. For the Pyrex cell, the frequency as a function of time is shown in Fig. 2 when the cell temperature was set to  $96^\circ\text{C}$  and the He pressure in the chamber was 0.65 atm. The temperature of the cell was actively stabilized to better than  $0.1^\circ\text{C}$ . The calculated slope  $(d\nu/dt)/\nu_0 = (\beta \times dP/dt)/\nu_0 = 7.6 \times 10^{-9} \text{ h}^{-1}$  (where  $\nu_0$  is the ground state hyperfine splitting of  $^{87}\text{Rb}$ ) corresponds to a permeation rate of about  $K_{\text{Pyrex}} = 3 \times 10^{-10} \text{ cm}^2/\text{s}$ . The same measurement was also done at  $106^\circ\text{C}$  and at  $116^\circ\text{C}$  [Fig. 2(b)], and as expected, the permeation rate is consistent with the Arrhenius equation, as can be seen in Fig. 2(c). Subsequently the Pyrex cell was replaced by another one made with ASG windows. This glass contains 15% to 20%  $\text{Al}_2\text{O}_3$  and is known to have a much lower permeation rate than Pyrex. The measurement of the frequency as a function of time at  $91^\circ\text{C}$  is shown in Fig. 3(a) when the helium pressure in the vacuum chamber was 0.56 atm. The slope is  $(d\nu/dt)/\nu_0 = 3.7 \times 10^{-11} \text{ h}^{-1}$ . The estimated ASG

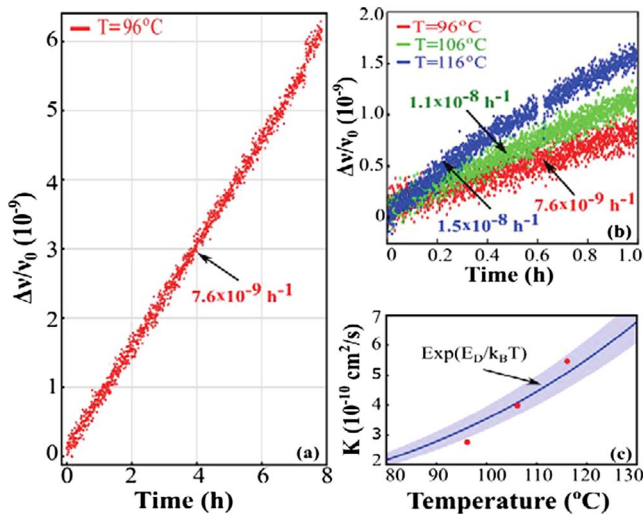


**Fig. 2.** (a) Change of the clock frequency as a function of time due to He diffusion in the cell at  $T_{\text{cell}} = 96^\circ\text{C}$  and  $P_{\text{He}} = 0.65$  atm for a cell having Pyrex windows. (b) The frequency change measured for two more temperatures ( $106^\circ\text{C}$  and  $116^\circ\text{C}$ ). (c) The permeation rate extracted from the frequency-shift data follows the Arrhenius equation. The blue band represents the uncertainty and accounts for the uncertainty in the cell temperature.

permeation rate was found to be  $K_{\text{ASG}} = 1.4 \times 10^{-12}$  cm<sup>2</sup>/s at  $91^\circ\text{C}$ . To confirm the measurement of the slope  $dP/dt$ , we measured the frequency drift at a higher temperature ( $110^\circ\text{C}$ ). At this temperature the contrast of the CPT signal was greatly reduced and it was difficult to accurately measure small changes in the clock frequency. In order to overcome this problem, we employed the following procedure. We heated the cell

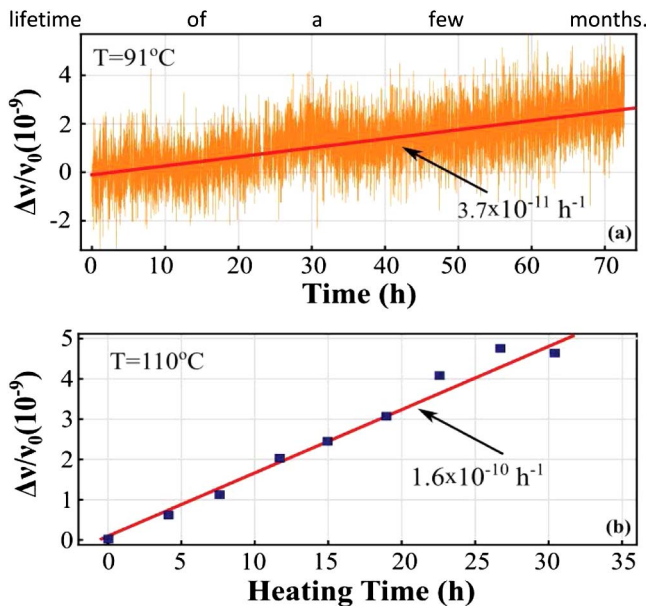


**Fig. 3.** (a) Change of the clock frequency as a function of time due to He diffusion in the cell at  $T_{\text{cell}} = 91^\circ\text{C}$  and  $P_{\text{He}} = 0.56$  atm for a cell having ASG windows. In (b) the temperature of the cell was altered between a low and a high value. The frequency change is determined by the He permeation rate at the highest temperature.

at  $110^\circ\text{C}$  for a certain amount of time [“heating time” axis in Fig. 3(b)] then we cooled down the cell at  $80^\circ\text{C}$  and we measured the clock frequency. We repeated this procedure several times. Because the diffusion and thus the permeation rate depend exponentially on temperature, the frequency change will mainly be caused by He permeation at  $110^\circ\text{C}$ . The result of this method is shown in Fig. 3(b). The slope in this case is about  $(d\nu/dt)/\nu_0 = 1.6 \times 10^{-10}$  h<sup>-1</sup> at  $110^\circ\text{C}$  and at 0.56 atm of He pressure. The estimated permeation rate is  $K_{\text{ASG}} = 6 \times 10^{-12}$  cm<sup>2</sup>/s at  $110^\circ\text{C}$ .

After completing the measurements of the frequency shift for the ASG at  $91^\circ\text{C}$  and  $110^\circ\text{C}$  we measured the laser power stability and we noticed that the laser power was slightly drifting. We also measured the light shift slope by changing the laser power by a known amount and measuring the frequency change. From the measured drift rate of the power (less than  $-0.1$  μW/h) and the light-shift slope ( $3.5$  Hz/μW) we can estimate that the frequency change due to the AC Stark shift is comparable to the one measured at  $91^\circ\text{C}$ . Because it is possible that the laser power was drifting slightly during the measurement at  $91^\circ\text{C}$ , it is possible that some or all of the measured frequency change over time is due to the slowly-varying AC Stark shift. Because the observed frequency drift at  $110^\circ\text{C}$  was 5 times larger than at  $91^\circ\text{C}$ , it is unlikely that the AC Stark shift contributed more than 20% to the drift rate at higher temperatures.

In order to compare the permeation rate of the Pyrex and the ASG glass at the same temperature we scale the diffusion constant measured at one temperature by  $e^{-E_D/k_B T}$ .  $E_D$  is known for Pyrex and we assume the value of  $E_D$  for Corning 1720 [4] to scale the ASG measurements. Thus at  $70^\circ\text{C}$ , which is within the operating temperature range of a CSAC cell, the permeation rate of the ASG is two orders of magnitude lower than that of Pyrex, whereas the permeation rate of Corning 1720 is four orders of magnitude lower than that of Pyrex. At  $25^\circ\text{C}$  the permeation rate of ASG is at least three orders of magnitude lower than that of Pyrex.

The change of helium pressure inside the cell as a function of time depends on the initial concentration of He in the glass windows. In Fig. 4 the pressure of the chamber is plotted according to Eq. (1) as a function of time for a completely degassed window and a nondegassed window [11], for which the initial He concentration is equal to the atmospheric concentration multiplied by the solubility. Window degassing is important to prevent rapid pressure rise after fabrication. For example if the cell is going to be used for laser cooling applications and only passive pumping elements like nonevaporable getters are going to be used [11], then the pressure inside the cell will rise above  $10^{-7}$  Torr almost immediately if Pyrex is used, in a few hours if SD2 is used and in a few days if Corning 1720 is used. If the windows are degassed prior to anodic bonding then the time needed for the pressure to rise above the  $10^{-7}$  Torr limit is significantly increased (few hours for Pyrex, few months for SD2 and many years for Corning 1720). The degassing of the material can be accomplished by placing the glass windows in a vacuum chamber and then heating them before bonding. The higher the heating temperature, the shorter the material has to remain in the chamber. For example if the heating temperature is set to  $200^\circ\text{C}$  then the ASG window will be completely degassed such that the remaining He in the glass will not cause the chamber

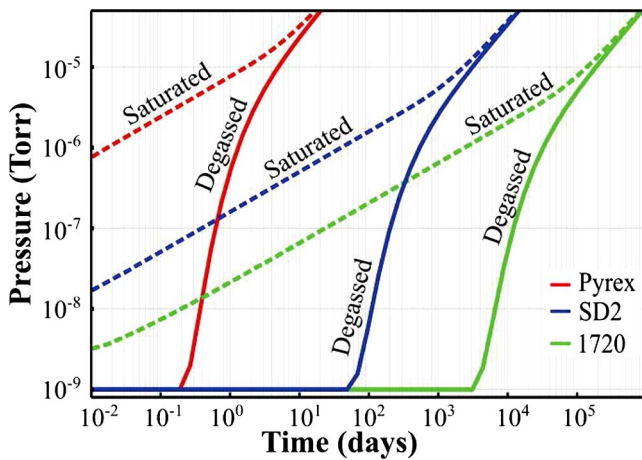


**Fig. 4.** Theoretical estimation of the pressure increases inside the cell due to He permeating the glass windows at 25°C. For the SD2, the value of the permeation rate comes from our measurements, while for the Corning 7740 and 1720 we used values from the literature [11].

pressure to rise above  $10^{-7}$  Torr over the lifetime of a few months.

We have identified an aluminosilicate type of glass that can be used for micro fabricated vapor cells. This type of glass has significantly lower permeation rate than Pyrex at room temperature. In addition to reducing the drift due to He permeation in vapor cell clocks, this glass may help enable highly miniaturized laser-cooled systems, for which a major obstacle is maintaining a good vacuum without using a large ion pump. The use of low-He-permeation glasses as described here may allow sufficiently good vacuums to be obtained with passive pumping methods such as getter pumps. A passively-pumped, micro fabricated cold atom platform would enable a new generation of compact, low-power cold atom precision instrumentation.

**Funding.** National Institute of Standards and Technology (NIST); DARPA's Microsystems Technology Office.

**Acknowledgment.** The views, opinions, and/or findings contained in this Letter are those of the authors and should not

be interpreted as representing the official views or policies of the Department of Defense or the U.S. Government.

## REFERENCES AND NOTE

1. T. P. Heavner, E. A. Donley, F. Levi, G. Costanzo, T. E. Parker, J. H. Shirley, N. Ashby, S. Barlow, and S. R. Jefferts, *Metrologia* **51**, 174 (2014).
2. I. K. Kominis, T. W. Kornack, J. C. Allred, and M. V. Romalis, *Nature* **422**, 596 (2003).
3. M. Arditi and T. R. Carver, *Phys. Rev.* **112**, 449 (1958).
4. F. J. Norton, *J. Am. Ceram. Soc.* **36**, 90 (1953).
5. K. J. Hughes, A. Sackett, C. A. Sackett, and A. T. Brown, "Helium barrier atom chamber," U.S. patent application 20,120,258,022 A1 (October 11, 2012).
6. J. C. Camparo, C. M. Klimcak, and S. J. Herbuloock, *IEEE Trans. Instrum. Meas.* **54**, 1873 (2005).
7. M. Bloch, O. Mancini, and T. McClelland, in *Proceedings of the IEEE International Frequency Control Symposium and PDA Exhibition* (IEEE, 2002), pp. 505–509.
8. A. B. Scholes, "Low helium permeability atomic frequency standard cell and method for forming same," U.S. patent application 5,256,995 A (October 26, 1993).
9. A. Ben-Amar Baranga, S. Appelt, M. Romalis, C. Erickson, A. Young, G. Cates, and W. Happer, *Phys. Rev. Lett.* **80**, 2801 (1998).
10. L. A. Liew, S. Knappe, J. Moreland, H. Robinson, L. Hollberg, and J. Kitching, *Appl. Phys. Lett.* **84**, 2694 (2004).
11. J. A. Rushton, M. Aldous, and M. D. Himsworth, *Rev. Sci. Instrum.* **85**, 121501 (2014).
12. T. Grzebyk, A. Górecka, and J. A. Dziuban, in *25th International Vacuum Nanoelectronics Conference* (IEEE, 2012), pp. 1–2.
13. S. Abdullah, C. Affolderbach, F. Gruet, and G. Miletì, *Appl. Phys. Lett.* **106**, 163505 (2015).
14. Products or companies named here are cited only in the interest of complete scientific description and neither constitute nor imply endorsement by NIST or by the U.S. government. Other products may be found to serve just as well.
15. G. Wallis and D. I. Pomerantz, *J. Appl. Phys.* **40**, 3946 (1969).
16. R. M. Barrer, *Diffusion in and through Solids* (The University Press/Macmillan, 1941).
17. W. A. Rogers, R. S. Buritz, and D. Alpert, *J. Appl. Phys.* **25**, 868 (1954).
18. V. O. Altemose, *J. Appl. Phys.* **32**, 1309 (1961).
19. S. Knappe, V. Shah, P. D. D. Schwindt, L. Hollberg, J. Kitching, L.-A. Liew, and J. Moreland, *Appl. Phys. Lett.* **85**, 1460 (2004).
20. J. Vanier and C. Audoin, *The Quantum Physics of Atomic Frequency Standards* (Adam Hilger, 1989).
21. R. Lutwak, A. Rashed, M. Varghese, G. Tepolt, J. Leblanc, M. Mescher, D. K. Serkland, and G. M. Peake, in *Proceedings of IEEE on International Frequency Control Symposium Joint Conference with the 21st European Frequency and Time Forum* (IEEE, 2007) pp. 1327–1333.